Mendeleev Communications

Mendeleev Commun., 2025, **35**, 82–85

Ultrafast processes in Fe^{III} complexes with malic and succinic acids in aqueous solutions

Ivan P. Pozdnyakov,*[a] Alexey A. Melnikov[b] and Sergey V. Chekalin[b]

[a] *V. V. Voevodsky Institute of Chemical Kinetics and Combustion, Siberian Branch of the Russian Academy of Sciences, 630090 Novosibirsk, Russian Federation. E-mail: ipozdnyak@kinetics.nsc.ru*

[b] *Institute of Spectroscopy, Russian Academy of Sciences, 142190 Troitsk, Moscow, Russian Federation*

DOI: 10.71267/mencom.7563

Femtosecond pump–probe spectroscopy is used to reveal photophysical processes in Fe^{III} complexes with two dicarboxylic acids (malic and succinic) in aqueous solutions. A model of primary photoprocesses is proposed that includes ultrafast vibrational cooling, solvent-mediated Franck–Condon excited-state relaxation and subsequent internal conversion to the ground state, accompanied by the formation of a long-lived Fe^{II} radical complex.

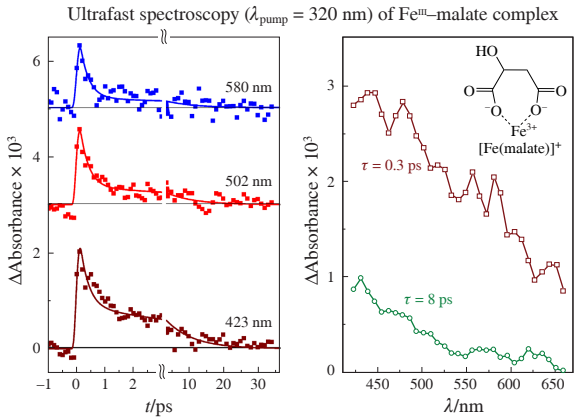

Keywords: Fe^{III} complexes, carboxylates, pump–probe spectroscopy, ultrafast processes, electron transfer, radical complexes.

Iron(III) complexes with simple carboxylic acids play an important role in the environmental photochemistry of the atmosphere and natural waters and are widely studied as potential photoactive agents for advanced oxidation processes (AOPs).[1–5] The photochemistry of some complexes with the simplest acids (oxalic, pyruvic, lactic, tartaric, citric *etc.*) has already been studied in detail, while compounds with more complex ligands have received much less attention.[6–14]

In our previous works, the nanosecond laser flash photolysis technique was used to clarify the mechanism of photolysis of Fe^{III}–carboxylate complexes upon LMCT excitation.[10–14] It was found that the main intermediate in the photochemistry of Fe^{III} complexes with several natural organic acids (tartaric, pyruvic, lactic, oxalic, glyoxalic, citric and glycolic) is the corresponding long-lived Fe^{II} radical complex formed as a result of electron transfer from the ligand to the Fe^{III} ion:

$$[Fe^{III}–OOC–R]^{2+} + h\nu \rightarrow [Fe^{II}\cdots{}^{\bullet}OOC–R]^{2+}. \quad (1a)$$

The radical complex has weak absorption bands in the visible region (maximum at 620–670 nm) and decays exponentially on a millisecond time scale (1–5 ms) *via* dissociation [reaction (2)] and reaction with dissolved oxygen [reaction (3)]. The dissociation of the radical complex leads to the escape of the organic radical into the bulk of the solution,[2,3] followed by its fast decarboxylation [reaction (4)].[9,11]

$$[Fe^{II}\cdots{}^{\bullet}OOC–R]^{2+} \rightarrow Fe^{2+} + RCO_2^{\bullet}, \quad (2)$$

$$[Fe^{II}\cdots{}^{\bullet}OOC–R]^{2+} + O_2 \rightarrow Fe^{2+} + RO_2^{\bullet} + CO_2, \quad (3)$$

$$RCO_2^{\bullet} \rightarrow R^{\bullet} + CO_2. \quad (4)$$

Secondary radicals $R^{\bullet}/RO_2^{\bullet}$ can react with different components of the system (*e.g.*, Fe^{III} complexes or molecular oxygen), determining the steady-state quantum yield of photolysis of Fe^{III} carboxylate.[9,11,12] Subsequently, reactive oxygen species ($O_2^{\bullet-}$, H_2O_2 and $^{\bullet}OH$) are formed, providing the means for oxidation and mineralization of organic contaminants in the aquatic environment.[1–3]

The long lifetime of radical complexes can be explained by a considerable elongation of the Fe–O bonds (the difference between the lengths of the Fe^{II}–O and Fe^{III}–O bonds is ~0.2 Å),[15] which leads to large structural changes in the Fe^{II}–radical complex and the formation of a potential barrier that prevents the back electron transfer. Another reason for the stability of radical complexes may be the ultrafast detachment of CO_2 after the electron transfer with the formation of the radical complex $[Fe^{II}\cdots{}^{\bullet}R]^{2+}$:

$$[Fe^{III}–OOC–R]^{2+} + h\nu \rightarrow [Fe^{II}\cdots{}^{\bullet}R]^{2+} + CO_2. \quad (1b)$$

This process has recently been invoked to interpret the results of infrared transient absorption spectroscopy experiments with the 1 : 3 Fe^{III}–oxalate complex, $[Fe(Ox)_3]^{3-}$. The characteristic CO_2 detachment times found in those studies were in the range of 400–500 fs.[17,18] However, it is unclear whether process (1b) occurs in radical complexes with other, more complex carboxylate ligands. In the following discussion, radical complexes will be understood as those that can be formed by processes (1a) or (1b). Indeed, the investigation of the primary stages in the photochemistry of Fe^{III}–carboxylate complexes is still a challenging task for experimentalists. Only a few publications on ultrafast spectroscopy of Fe^{III} carboxylates, in particular the $[Fe(Ox)_3]^{3-}$ complex, can be found in the

literature.[15–19] It is believed that excitation of the $[Fe(Ox)_3]^{3-}$ complex leads to immediate (<30 fs) photoreduction of the central ion due to electron transfer with the formation of a short-lived excited state $[Fe^{II}(Ox)_3]^{*3-}$.[19] The latter rapidly releases CO_2 with the formation of primary radical complex of Fe^{II} with a coordinated $CO_2^{\bullet-}$ fragment [reaction (5)].

$$[Fe(Ox)_3]^{3-} + h\nu \rightarrow [(Ox)_2Fe^{II}\cdots(CO_2^{\bullet-})]^{3-} + CO_2. \quad (5)$$

This radical complex isomerizes and releases the $CO_2^{\bullet-}$ radical into the bulk on a time scale of hundreds of picoseconds to form the final complex $[Fe^{II}(Ox)_2]^{2-}$.[18] The $CO_2^{\bullet-}$ radical then readily reacts with a second complex $[Fe(Ox)_3]^{3-}$. This mechanism could explain the high quantum yield of photolysis of this complex, greater than unity.[8] However, this interpretation[17–18] is inconsistent with the results of laser flash photolysis experiments (see ref. 10 and references therein), in which long-lived intermediates (various Fe^{II} radical complexes) were observed on micro- and millisecond time scales. Therefore, the mechanism of the primary stage of photolysis of Fe^{III}–carboxylates is still unclear.

In this work, we investigate the photophysical properties of aqueous solutions of 1 : 1 Fe^{III} complexes with two dicarboxylic acids (malic and succinic) using femtosecond pump–probe spectroscopy. Malic and succinic acids differ from oxalic acid by the presence of two $–CH_2–$ fragments between two carboxyl groups of the ligand. Malic acid differs from succinic acid by an additional OH group in the aliphatic chain, while both acids are structurally close to the already studied tartaric acid[16] containing two OH groups in the aliphatic chain (Figure 1). Data on the spectroscopic and photochemical properties of these complexes are scarce, and only the quantum yields of their stationary photolysis can be found in the literature.[9,20] The main attention was paid to determining the origin, as well as the spectral and kinetic parameters of the excited states of the complexes and comparing these parameters with the available data for similar Fe^{III} carboxylates.†

Excitation of the LMCT transition in the $[Fe(malate)]^+$ complex by a femtosecond laser pulse leads to the formation of transient absorption, which almost completely decays within 30 ps (Figure 2). The kinetic curves at several selected wavelengths are presented in Figure 2(*b*). Global analysis of the temporal profile in the wavelength range of 410–660 nm by the iterative deconvolution method shows that the use of the biexponential function (6) with a Gaussian IRF provides a good fit with the time constants $\tau_1 = 0.3$ ps and $\tau_2 = 8$ ps.

$$\Delta A(\lambda,t) = A_1(\lambda)e^{-\frac{t}{\tau_1}} + A_2(\lambda)e^{-\frac{t}{\tau_2}}. \quad (6)$$

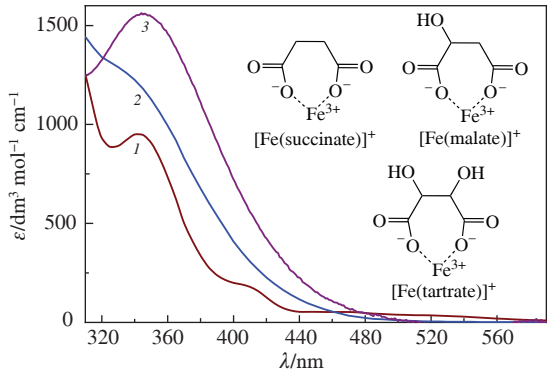

Figure 1 Absorption spectra and chemical structures of Fe^{III} complexes with (*1*) succinic, (*2*) malic and (*3*) tartaric[16] acids. Conditions: (*1*) $[Fe^{III}] = 6.7$ mM, [succinate] = 14 mM, pH 3.5; (*2*) $[Fe^{III}] = 6.7$ mM, [malate] = 10 mM, pH 2.5.

For the $[Fe(succinate)]^+$ complex, the ultrafast dynamics is rather similar to that observed for the $[Fe(malate)]^+$ complex. The transient absorption decays almost completely within 250 ps with two characteristic time constants: $\tau_1 = 0.6$ ps and $\tau_2 = 70$ ps (Figure 3). Such two-stage dynamics with comparable time constants was also observed previously for Fe^{III}–carboxylate complexes with tartaric, lactic and citric acids.[16] For example, for the $[Fe(tartrate)]^+$ complex, the calculated time constants τ_1

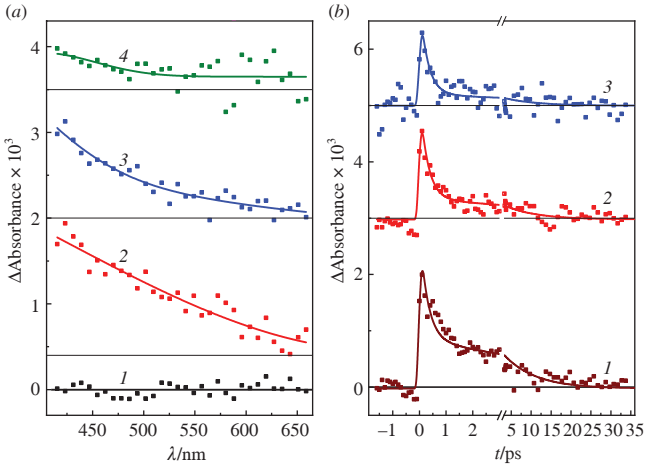

Figure 2 Femtosecond photolysis ($\lambda_{pump} = 320$ nm) of the $[Fe(malate)]^+$ complex: (*a*) transient absorption spectra at delay times of (*1*) –1, (*2*) 0.4, (*3*) 1.0 and (*4*) 3.3 ps between the probe and pump pulses; (*b*) kinetic curves at wavelengths of (*1*) 423, (*2*) 502 and (*3*) 580 nm. Solid lines are the best biexponential fits after deconvolution with IRF.

† Malic acid (Merck, 99%), succinic acid (Aldrich, 98%) and Fe^{III} perchlorate hydrate (Aldrich) were used without further purification. Perchloric acid (chemically pure, Reachem, Russia) and sodium hydroxide (chemically pure, Reachem, Russia) were used to adjust the pH of the solutions. Water was deionized using an Ultra Clear UV plus TM water purification system (SG water, Germany) to a quality of 18.2 MΩ cm and used to prepare all the solutions studied in the experiments. The absorption spectra of the samples were recorded using Shimadzu UV 2501 PC and Agilent HP8453 spectrophotometers. The composition of Fe^{III} complexes was calculated using Visual MINTEQ software (ver. 3.1).[21] Complexes $[Fe(malate)]^+$ and $[Fe(succinate)]^+$ were prepared by mixing Fe^{III} perchlorate solutions with solutions of the corresponding organic acids at the appropriate pH. Under all conditions used, more than 90% of Fe^{III} existed as the corresponding 1 : 1 complex. The shape of the spectra (see Figure 1) and the absorption coefficients {$\lambda_{max} = 335$ nm ($\varepsilon_{max} = 1300$ dm^3 mol^{-1} cm^{-1}) for $[Fe(malate)]^+$ and $\lambda_{max} = 345$ nm ($\varepsilon_{max} = 1000$ dm^3 mol^{-1} cm^{-1}) for $[Fe(succinate)]^+$} are consistent with the data available in the literature.[9]

The ultrafast visible transient absorption spectroscopy experiments were performed using a setup described elsewhere.[22] The initial source of femtosecond pulses at 800 nm was a Tsunami Ti:sapphire laser oscillator–Spitfire Pro regenerative amplifier system (Spectra Physics). The samples were excited at 320 nm (the 4th harmonic of the signal wave of TOPAS parametric amplifier); the pump pulse energy was ~1 μJ at a repetition rate of 1 kHz. Such a low energy was used to suppress the so-called 'coherent artifact' formed due to the interaction of the pump and probe pulses. The instrument response time of the transient absorption spectroscopy setup was about 200 fs. The excitation wavelength falls within the broad LMCT band of the complexes.[23] A portion of the 800 nm laser beam was focused into a cell containing flowing water to generate supercontinuum, which was used for probing.

The samples were placed in a 1 mm thick circular rotating cell (total volume of 1 ml) to ensure uniform irradiation of the solution and to avoid unwanted thermal effects caused by the pump pulse. Sample degradation after each measurement did not exceed 10%. ExciPro software (CDP Systems) was used to account for the group delay dispersion in the numerical preprocessing of the acquired time-resolved spectra. The corrected experimental data (32 kinetic curves at specific wavelengths) were globally fitted to a single set of kinetic parameters using PigSpec software, which allows modeling the instrument response function (IRF) as a Gaussian pulse. Typically, a biexponential function was used for fitting.

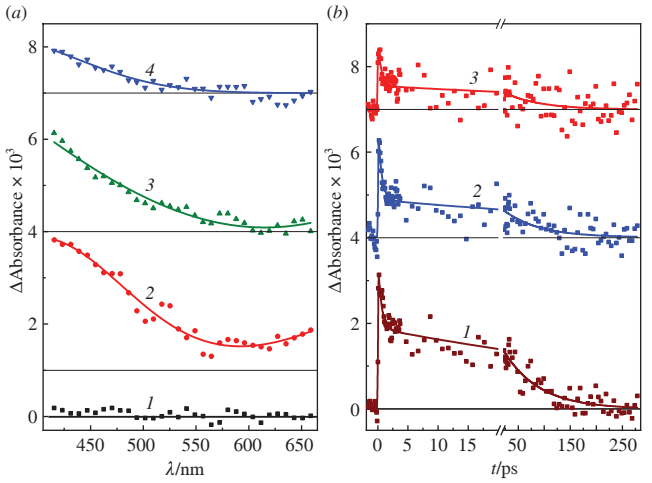

Figure 3 Femtosecond photolysis (λ_{pump} = 320 nm) of the [Fe(succinate)]$^+$ complex: (*a*) transient absorption spectra at delay times of (*1*) –1, (*2*) 0.4, (*3*) 3 and (*4*) 37 ps between the probe and pump pulses; (*b*) kinetic curves at wavelengths of (*1*) 423, (*2*) 502 and (*3*) 580 nm. Solid lines are the best biexponential fits after deconvolution with IRF.

and τ_2 were 1.0 and 40 ps, respectively. It is worth noting that there is no clear relationship between the number of OH groups (0, 1 or 2) in the aliphatic chain and the characteristic times of ultrafast processes in the corresponding complexes, since they all fall within the same time windows (0.3–1 ps for τ_1 and 8–70 ps for τ_2).

Using the calculated amplitude spectra of the temporal components $A_1(\lambda)$ and $A_2(\lambda)$, the transient absorption spectra can be constructed at specific delay times for both complexes (Figure 4). Immediately after the excitation (zero delay time, sum of the amplitudes), the spectrum demonstrates a broad absorption band with a maximum at a wavelength shorter than 410 nm. After the end of the first fast process (τ_1), the absorption band clearly shifts towards shorter wavelengths (amplitude A_2). A similar spectral evolution was previously observed for closely related Fe^{III}–carboxylate complexes.[16]

It is worth noting that the characteristic absorption bands of radical complexes detected during nanosecond laser flash photolysis of similar Fe^{III} carboxylates (λ_{max} = 620–650 nm) were not observed in these femtosecond experiments due to the extremely low absorption coefficients of the radical complexes (<100 dm^3 mol^{-1} cm^{-1}).[11–14] However, we believe that in our case these radical complexes nevertheless arise, by analogy with the systems already studied.[12,14,16]

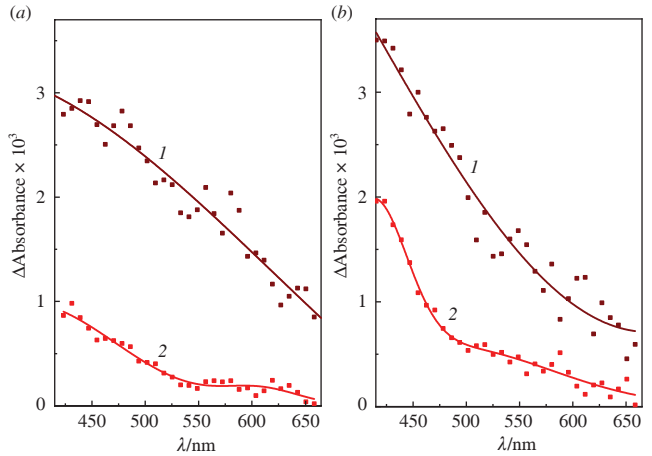

Figure 4 Global analysis of experimental kinetic curves for (*a*) [Fe(malate)]$^+$ and (*b*) [Fe(succinate)]$^+$ complexes: transient absorption spectra (*1*) at zero delay time [sum of amplitudes $A_1(\lambda)+A_2(\lambda)$] and (*2*) at the end of ultrafast relaxation [amplitude $A_2(\lambda)$].

The ground state multiplicity of the [Fe(malate)]$^+$ and [Fe(succinate)]$^+$ complexes is not reported in the literature, but it can assumed to be equal to 2, as for the $[Fe(Ox)_3]^{3-}$ complex. The latter is a low-spin complex with a large crystal field splitting due to the strong field of the oxalate ligands. It is also known that the quantum yield of Fe^{II} formed during photolysis of Fe^{III} complexes with well-studied dicarboxylic acids depends rather weakly on the excitation wavelength (λ_{ex}) and is 1.25 for the Fe^{III}–oxalate complex (λ_{ex} = 260–365 nm[24]) and ~0.4 for the Fe^{III}–tartrate complex (λ_{ex} = 313,[20] 355[11] and 366[20] nm), respectively. This fact indicates that the formation of the Fe^{II} radical complex occurs from the thermalized excited state of the corresponding Fe^{III}–carboxylate.

The similarity of the spectral evolution and calculated time constants for the Fe^{III} complexes of malic and succinic acids with those for previously studied systems allows us to explain the two-stage dynamics observed for Fe^{III}–carboxylate complexes upon excitation of the charge transfer band by the following mechanism.[16,25]

The first process with the time constant τ_1 can be identified with the combination of ultrafast vibrational cooling and solvent relaxation of the Franck–Condon excited state (^{2}LMCT) to the thermalized state (Figure 5). It can be expected that the relaxation of the Franck–Condon excited state will lead to some narrowing of the absorption band due to vibrational relaxation[26] and a blue shift of the absorption maximum due to the so-called dynamic Stokes shift,[27] which was indeed observed experimentally (see Figure 4). The thermalized excited state decays with the time constant τ_2 *via* two processes, namely, internal conversion to the ground state (k_{IC}) and the formation of a long-lived Fe^{II} radical complex (k_{RC}). The competition of these processes determines the high quantum yield of photolysis (ϕ_{phot}) of Fe^{III}–carboxylates (see Figure 5).

Another possible mechanism could be related to the intersystem crossing[28,29] from the ^{2}LMCT state to the low-lying metal-centered ^{4,6}MC state with higher multiplicity.[29] This process is also ultrafast and can take less than 1 ps in the case of metal complexes.[25,28,29] However, this mechanism is not discussed in the context of the photochemistry of Fe^{III} carboxylates. Moreover, this mechanism cannot explain the high yield of Fe^{II} radical complexes observed in the nanosecond laser flash photolysis experiments.[10–14] Thus, we believe that the model presented in Figure 5 provides a more consistent interpretation of the femtochemistry of the studied Fe^{III} complexes.

In summary, femtosecond pump–probe spectroscopy was used to identify ultrafast photophysical processes in Fe^{III} complexes with two dicarboxylic acids (malic and succinic) in aqueous solutions. We proposed a mechanism of primary photoprocesses that involves ultrafast vibrational cooling and solvent relaxation of the Franck–Condon excited state and

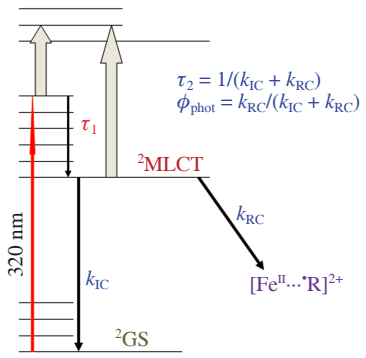

Figure 5 Jablonski diagram showing the primary relaxation stages of the studied Fe^{III} complexes and the formation of the Fe^{II} radical complex.

superposition of internal conversion to the ground state and formation of a long-lived Fe^{II} radical complex. The obtained results describing the primary stages of photolysis of the studied complexes are important for formulating a general mechanism of photolysis of natural Fe^{III} carboxylates, which play an important role in environmental photochemistry and can be applied for the development of AOPs. Further understanding of the photochemistry of the studied complexes requires detection of radical complexes by laser flash photolysis and determination of quantum yields of photolysis of the complexes in stationary photochemical experiments.

The financial support from the Russian Science Foundation (grant no. 23-23-00097) is gratefully acknowledged.

References

1 K. Barbeau, *Photochem. Photobiol.*, 2006, **82**, 1505; https://doi.org/10.1111/j.1751-1097.2006.tb09806.x.
2 Y. Zuo and J. Hoigné, *Environ. Sci. Technol.*, 1992, **26**, 1014; https://doi.org/10.1021/es00029a022.
3 F. Wu and N. Deng, *Chemosphere*, 2000, **41**, 1137; https://doi.org/10.1016/S0045-6535(00)00024-2.
4 *Advanced Oxidation Processes for Wastewater Treatment: Emerging Green Chemical Technology*, eds. S. C. Ameta and R. Ameta, Academic Press, London, 2018; https://doi.org/10.1016/C2016-0-00384-4.
5 M. Sievers, in *Treatise on Water Science*, ed. P. Wilderer, Elsevier, Amsterdam, 2011, vol. 4, pp. 377–408; https://doi.org/10.1016/B978-0-444-53199-5.00093-2.
6 L. Clarizia, D. Russo, I. Di Somma, R. Marotta and R. Andreozzi, *Appl. Catal., B*, 2017, **209**, 358; https://doi.org/10.1016/j.apcatb.2017.03.011.
7 P. Kocot, A. Karocki and Z. Stasicka, *J. Photochem. Photobiol., A*, 2006, **179**, 176; https://doi.org/10.1016/j.jphotochem.2005.08.016.
8 C. Weller, S. Horn and H. Herrmann, *J. Photochem. Photobiol., A*, 2013, **255**, 41; https://doi.org/10.1016/j.jphotochem.2013.01.014.
9 C. Weller, S. Horn and H. Herrmann, *J. Photochem. Photobiol., A*, 2013, **268**, 24; https://doi.org/10.1016/j.jphotochem.2013.06.022.
10 I. P. Pozdnyakov, O. V. Kel, V. F. Plyusnin, V. P. Grivin and N. M. Bazhin, *J. Phys. Chem. A*, 2008, **112**, 8316; https://doi.org/10.1021/jp8040583.
11 E. M. Glebov, I. P. Pozdnyakov, V. P. Grivin, V. F. Plyusnin, X. Zhang, F. Wu and N. Deng, *Photochem. Photobiol. Sci.*, 2011, **10**, 425; https://doi.org/10.1039/c0pp00151a.
12 I. P. Pozdnyakov, Y. E. Tyutereva, A. V. Mikheilis, V. P. Grivin and V. F. Plyusnin, *J. Photochem. Photobiol., A*, 2023, **434**, 114274; https://doi.org/10.1016/j.jphotochem.2022.114274.
13 F. Wu, N. Deng, E. M. Glebov, I. P. Pozdnyakov, V. P. Grivin, V. F. Plyusnin and N. M. Bazhin, *Russ. Chem. Bull.*, 2007, **56**, 900; https://doi.org/10.1007/s11172-007-0136-7.
14 I. P. Pozdnyakov, F. Wu, A. A. Melnikov, V. P. Grivin, N. M. Bazhin, S. V. Chekalin and V. F. Plyusnin, *Russ. Chem. Bull.*, 2013, **62**, 1579; https://doi.org/10.1007/s11172-013-0227-6.
15 J. Chen, H. Zhang, I. V. Tomov, M. Wolfsberg, X. Ding and P. M. Rentzepis, *J. Phys. Chem. A*, 2007, **111**, 9326; https://doi.org/10.1021/jp0733466.
16 I. P. Pozdnyakov, A. A. Melnikov, N. Tkachenko, S. V. Chekalin, H. Lemmetyinen and V. F. Plyusnin, *Dalton Trans.*, 2014, **43**, 17590; https://doi.org/10.1039/C4DT01419G.
17 D. M. Mangiante, R. D. Schaller, P. Zarzycki, J. F. Banfield and B. Gilbert, *ACS Earth Space Chem.*, 2017, **1**, 270; https://doi.org/10.1021/acsearthspacechem.7b00026.
18 S. Straub, P. Brünker, J. Lindner and P. Vöhringer, *Phys. Chem. Chem. Phys.*, 2018, **20**, 21390; https://doi.org/10.1039/C8CP03824D.
19 L. Longetti, T. R. Barillot, M. Puppin, J. Ojeda, L. Poletto, F. van Mourik, C. A. Arrell and M. Chergui, *Phys. Chem. Chem. Phys.*, 2021, **23**, 25308; https://doi.org/10.1039/D1CP02872C.
20 H. B. Abrahamson, A. B. Rezvani and J. G. Brushmiller, *Inorg. Chim. Acta*, 1994, **226**, 117; https://doi.org/10.1016/0020-1693(94)04077-X.
21 [dataset] J. P. Gustafsson, *Visual MINTEQ: A freeware chemical equilibrium model for the calculation of metal speciation, solubility equilibria, sorption* etc. *for natural waters*, version 3.1, 2024; https://vminteq.com/download/.
22 S. V. Chekalin, *Phys.-Usp.*, 2006, **49**, 634; https://doi.org/10.1070/PU2006v049n06ABEH006044.
23 V. Balzani and V. Carassiti, *Photochemistry of Coordination Compounds*, Academic Press, London, 1970; https://archive.org/details/photochemistryof0000balz/page/n7/mode/2up?view=theater.
24 S. Goldstein and J. Rabani, *J. Photochem. Photobiol., A*, 2008, **193**, 50; https://doi.org/10.1016/j.jphotochem.2007.06.006.
25 A. Vlček, Jr., *Coord. Chem. Rev.*, 2000, **200–202**, 933; https://doi.org/10.1016/S0010-8545(00)00308-8.
26 E. A. Juban and J. K. McCusker, *J. Am. Chem. Soc.*, 2005, **127**, 6857; https://doi.org/10.1021/ja042153i.
27 A. Pigliucci, G. Duvanel, L. M. Lawson Daku and E. Vauthey, *J. Phys. Chem. A*, 2007, **111**, 6135; https://doi.org/10.1021/jp069010y.
28 A. Cadranel, L. Gravogl, D. Munz and K. Meyer, *Chem. – Eur. J.*, 2022, **28**, e202200269; https://doi.org/10.1002/chem.202200269.
29 G. I. Zhdankin, I. P. Pozdnyakov, A. V. Mikheylis, V. P. Grivin, D. B. Vasilchenko, A. A. Melnikov, S. V. Chekalin and E. M. Glebov, *Mendeleev Commun.*, 2024, **34**, 488; https://doi.org/10.1016/j.mencom.2024.06.006.

Received: 2nd July 2024; Com. 24/7563